

# Real Time Flow Rate Estimation in Injection Molding

*Bingfeng Fan, David Kazmer, and Ranjan Mukhari  
Department of Plastics Engineering  
University of Massachusetts Lowell  
1 University Avenue  
Lowell, MA 01854*

## Abstract

Plastics injection molding has been limited by the lack of observability and controllability, such that it has not been possible to know or control flow rates and pressures at multiple locations in a mold. An instrumentation and analysis method is presented that allows the estimation of flow rate and pressure at multiple points in an injection mold. The instrumentation consists of melt pressure transducers at the inlet and outlets of the feed system, and optionally the inlet flow rate. A non-Newtonian, non-isothermal, faster than real time simulation utilizes this feedback to estimate the flow rates delivered through each branch of the feed system, and also provide feedback regarding the apparent viscosity of the polymer melt provided by the molding machine. Validation results are provided for a two-cavity mold with a valve-gated hot runner system.

## Introduction

There has been a sustained evolution towards closed loop control in injection molding. Advances are driven largely by economic concerns since machines can typically operate at higher production rates and with high production yields under closed loop control than with open loop control. By definition, every closed loop control loop requires a feedback path back to the output being controlled. Most closed loop controls act on feedback regarding machine elements, which do not necessarily provide precise control of the process states that determine the quality of molded products. In fact, with respect to the quality of molded parts, injection molding is not a closed loop process. Instead, injection molding is an open loop process in which many closed loop processes are linked such that the consistency of the molded products is (hopefully) very high [1].

This paper strives to improve the observability of the injection molding process by ‘fusing’ information from the molding machine, sensors in the injection mold, and real time flow analysis. As a result, the flow rates and pressures at multiple locations in an injection mold can be estimated via a faster than real time simulation and used for real time control. The results are useful in several ways, including but not limited to:

- Estimation of cavity pressure from upstream sensors, which may be more economical or robust than those placed in the mold;

- Estimation of flow rates through multiple branches and gates in a feed system;
- Use of estimated flow rates and pressures for quality control;
- Use of estimated flow rates and pressures for real time process control with adjustable valves, thereby enabling each valve to provide distinct filling and packing stages;
- Use of redundant information to estimate changes in the melt.

This work builds on several past endeavors, including those related to cavity pressure sensing [2-5], sensor fusion [6], on-line rheometry [7-9], injection molding process simulation [10-16], process development [17, 18], process control [19, 20], and process optimization [21-25]. Given space limitations, the reader is provided the references to consult as interested.

The paper progresses as follows. First, the concept of flow networks is presented with Newtonian flow as an illustration. Second, an on-line simulation for the analysis of flow networks with non-Newtonian, non-isothermal, compressible fluids is presented. Finally, the results of the non-Newtonian, non-isothermal flow network analysis are validated against experimental observations.

## Flow Networks

The feed system in injection molds can be modeled as a flow network. This research is directed to providing estimates of melt flow rates and pressures at varying locations in the network. Consider a Newtonian fluid in a rod. The relationship between flow rate and pressure gradient can be modeled as [26, 27]

$$Q = \frac{\pi R^4 \Delta P}{8 \mu L} \quad (1)$$

where  $Q$  is the volumetric flow rate,  $R$  is the rod radius,  $\Delta P$  is the pressure drop,  $\mu$  is the apparent viscosity, and  $L$  is the length of the rod. With the relationship between flow rate and pressure gradient known for each segment of the flow network, a flow conductance matrix,  $\mathbf{K}$ , may be utilized to relate the vector of flow rates,  $\mathbf{Q}$ , to the vector of pressures,  $\mathbf{P}$ :

$$\mathbf{Q} = \mathbf{K}\mathbf{P} \quad (2)$$

For any node in the network, the inlet flow rates are considered positive, and the outlet flow rates are considered negative. Any flow rate  $Q_i$  in the flow rate vector  $\mathbf{Q}$  is the algebraic sum of all inlet and outlet flow rates for that node. As an example, consider the flow network shown in Figure 1. Each segment of the feed system can be thought of as an “element”, which is typically either a rod or an annulus with two end nodes, node  $i$  and node  $j$ , and an associate conductance coefficient  $k_{ij}$ , such that

$$k_{ij}(P_j - P_i) = Q_i \quad (3)$$

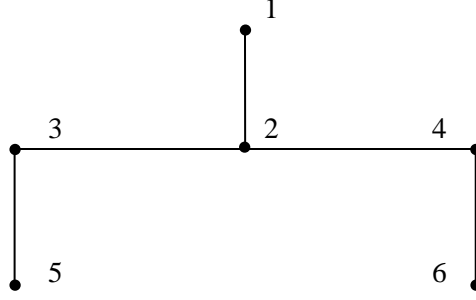


**Figure 1** Flow network

Each node of the element has an algebraic flow rate. By assembling the element conductance matrix and the element flow rate vector, a global conductance equation as Eq. 2 is obtained:

$$\begin{bmatrix} Q_1 \\ Q_2 \\ Q_3 \\ Q_4 \\ Q_5 \\ Q_6 \end{bmatrix} = \begin{bmatrix} -k_{12} & k_{12} & 0 & 0 & 0 & 0 \\ k_{12} & -k_{12} - k_{23} - k_{24} & k_{23} & k_{24} & 0 & 0 \\ 0 & k_{23} & -k_{23} - k_{35} & 0 & k_{35} & 0 \\ 0 & k_{24} & 0 & -k_{24} - k_{46} & 0 & k_{46} \\ 0 & 0 & k_{35} & 0 & -k_{35} & 0 \\ 0 & 0 & 0 & k_{46} & 0 & -k_{46} \end{bmatrix} \begin{bmatrix} P_1 \\ P_2 \\ P_3 \\ P_4 \\ P_5 \\ P_6 \end{bmatrix} \quad (4)$$

Consider an injection molding process where the pressures at the inlet ( $P_1$ ) and each of the gates ( $P_5$ , and  $P_6$ ) are known. Conservation of mass requires the net flow rate at points 2, 3, and 4 to be zero. There are six remaining unknown quantities, which may be solved via the six equations provided by the flow conductance matrix:

$$\begin{bmatrix} Q_1 \\ 0 \\ 0 \\ 0 \\ Q_5 \\ Q_6 \end{bmatrix} = \begin{bmatrix} -k_{12} & k_{12} & 0 & 0 & 0 & 0 \\ k_{12} & -k_{12} - k_{23} - k_{24} & k_{23} & k_{24} & 0 & 0 \\ 0 & k_{23} & -k_{23} - k_{35} & 0 & k_{35} & 0 \\ 0 & k_{24} & 0 & -k_{24} - k_{46} & 0 & k_{46} \\ 0 & 0 & k_{35} & 0 & -k_{35} & 0 \\ 0 & 0 & 0 & k_{46} & 0 & -k_{46} \end{bmatrix} \begin{bmatrix} P_1^{obs} \\ P_2 \\ P_3 \\ P_4 \\ P_5^{obs} \\ P_6^{obs} \end{bmatrix} \quad (5)$$

For Newtonian fluids, the coefficients in the conductance matrix may be estimated analytically via Eq. 1. However, polymer melt flow is known to be non-Newtonian, and furthermore the shear heating effect renders the flow condition non-isothermal even for the hot runner systems. Therefore, the flow conductance equation Eq. 2 is non-linear, and the accuracy of analytical methods for developing the conductance matrix may be compromised [28]. Accordingly, an iterative solution process is necessary to better calculate the flow conductance coefficients, entailing a numerical simulation which will be discussed in the next section.

## Numerical Simulation

One motivation of the numerical simulation is to calculate the coefficients of the flow conductance matrix. Two geometries are most common in the hot runner systems of injection molding: 1) rod and 2) annulus. Both geometries are modeled as 1-D axisymmetric flow field consistent with our previous efforts [29], following the methodology of Chiang [30].

### *Mathematical modeling*

For the modeling of rods and annuli, the governing equations are the same. The only difference is the boundary conditions. The continuity equation, momentum equation, and energy equation for non-isothermal polymer creep flow in cylindrical coordinates are given by

$$\frac{\partial \rho}{\partial t} + \frac{\partial}{\partial z}(\rho u) = 0 \quad (6)$$

$$\frac{1}{r} \frac{\partial}{\partial r} \left( r \eta \frac{\partial u}{\partial r} \right) = \frac{\partial p}{\partial z} \quad (7)$$

$$\rho C_p \left( \frac{\partial T}{\partial t} + u \frac{\partial T}{\partial z} \right) = \frac{1}{r} \frac{\partial}{\partial r} \left( r k \frac{\partial T}{\partial r} \right) + \eta \dot{\gamma}^2 \quad (8)$$

where  $\rho$  is density, and  $u$  is the velocity,  $C_p$  is specific heat,  $T$  is temperature  $k$  is the thermal conductivity,  $\eta$  is the viscosity and  $\dot{\gamma}$  is the shear rate. The boundary conditions for flow in rods are:

$$u = 0 \quad T = T_{w2} \quad \text{at } r = R_2 \quad (9)$$

$$\frac{\partial u}{\partial r} = \frac{\partial T}{\partial r} = 0 \quad \text{at } r = 0 \quad (10)$$

The boundary conditions for flow in annuli are:

$$u = 0 \quad T = T_{w2} \quad \text{at } r = R_2 \quad (11)$$

$$u = 0 \quad T = T_{w1} \quad \text{at } r = R_1 \quad (12)$$

where  $R_1$  and  $R_2$  are the inner and outer radii respectively ( $R_1 = 0$  for rods), and  $T_{w1}$  and  $T_{w2}$  are the wall temperatures at the inner and outer radii.

Integrating Eq. 7 once,

$$r \eta \frac{\partial u}{\partial r} = \frac{\partial p}{\partial z} \frac{r^2}{2} + C_1 \quad (13)$$

For rods, applying the boundary condition Eq. 10 results in

$$\frac{\partial u}{\partial r} = \frac{1}{\eta} \frac{\partial p}{\partial z} \frac{r}{2} \quad (14)$$

Integrating Eq. 14 from  $r$  to  $R_2$  and applying the boundary condition Eq. 9 results in

$$u = \int_r^{R_2} -\frac{\partial p}{\partial z} \frac{\hat{r}}{2\eta} d\hat{r} \quad (15)$$

For annuli, integrating Eq. 14 from  $r$  to  $R_2$  and applying the boundary condition Eq. 12 results in

$$u = \int_r^{R_2} -\frac{\partial p}{\partial z} \frac{\hat{r}}{2\eta} d\hat{r} - \int_r^{R_2} \frac{C_1}{\eta \hat{r}} d\hat{r} \quad (16)$$

Applying the boundary condition Eq. 11 results in

$$u = -\frac{\partial p}{\partial z} \int_r^{R_2} \left( \frac{\hat{r}}{2\eta} - \frac{\lambda}{\eta \hat{r}} \right) d\hat{r} \quad (17)$$

where

$$\lambda = \int_{R_1}^{R_2} \frac{\hat{r} d\hat{r}}{2\eta} / \int_r^{R_2} \frac{d\hat{r}}{\eta \hat{r}} \quad (18)$$

The volumetric flow rate is given by

$$Q = 2\pi \int_{R_1}^{R_2} u r dr = 2\pi \left( -\frac{\partial p}{\partial z} \right) \tilde{S} \quad (19)$$

where for rods,  $\tilde{S} = \int_0^{R_2} \rho \left( \int_r^{R_2} \frac{\hat{r} d\hat{r}}{2\eta} \right) r dr$ , and for annuli,  $\tilde{S} = \int_{R_1}^{R_2} \rho \left( \int_r^{R_2} \left( \frac{\hat{r}}{2\eta} - \frac{\lambda}{\eta \hat{r}} \right) d\hat{r} \right) r dr$ .

The temperature field is obtained by solving the energy equation Eq. 8 via a finite difference method. The viscosity model is Cross-WLF (ref. Chiang).

### *Numerical algorithm*

As mentioned in the previous section, for injection molding, the coefficients in the conductance matrix have to be estimated via numerical iteration. The details of the algorithm are as follows. At each time step, the temperature field is calculated by the finite difference method from the energy equation. Then, the viscosity is calculated with the temperature field and the shear rate information from the previous time step. For each element, the conductance coefficient is first estimated via

$$k_{ij} = \frac{\pi R_2^4}{8\eta L} \text{ for rods} \quad (20)$$

$$\text{and } k_{ij} = \frac{\pi R_2^4}{8\eta L} \left[ (1 - \kappa^2) - \frac{(1 - \kappa^2)^2}{\ln(1/\kappa)} \right] \text{ for annuli} \quad (21)$$

where  $\eta$  is the viscosity chosen at the center of the rod or the gap between the inner and outer radii of annuli.

Afterwards, the global conductance matrix  $\mathbf{K}$  is assembled. The known pressures and flow rates can be given in arbitrary combinations of  $P_i$  and  $Q_i$ , as long as the number of unknowns is equal to the number of nodes. With the estimated coefficients, the unknown pressure variables are calculated from the flow conductance equation, Eq. 2. When all pressures are known, the coefficients of the flow conductance matrix is updated by

$$k_{ij} = 2\pi\tilde{S} / L \quad (22)$$

where  $\tilde{S}$  is the variable obtained from Eq. 19. With the new coefficients, recalculate the pressure and flow rate unknowns. This process proceeds until the change of the pressure unknowns is negligible.

## Validation

Experiments were conducted with a two-cavity mold having a valve-gated hot runner system produced by Mold-Masters, Ltd of Georgetown, Ontario. The mold was constructed having two cavities for producing binder separators, wherein each cavity utilized exchangeable mold inserts for shutting off the flow. Figure 2 shows the hot runner system geometry, a full binder part, and a partial binder part with a significantly longer flow length.

It is very important to understand that while the flow rates in the physical system are dependent on the geometry of both the feed system and mold cavity, the on-line estimation of the flow rate requires only the feed system geometry along with sensor data indicative of the boundary conditions.

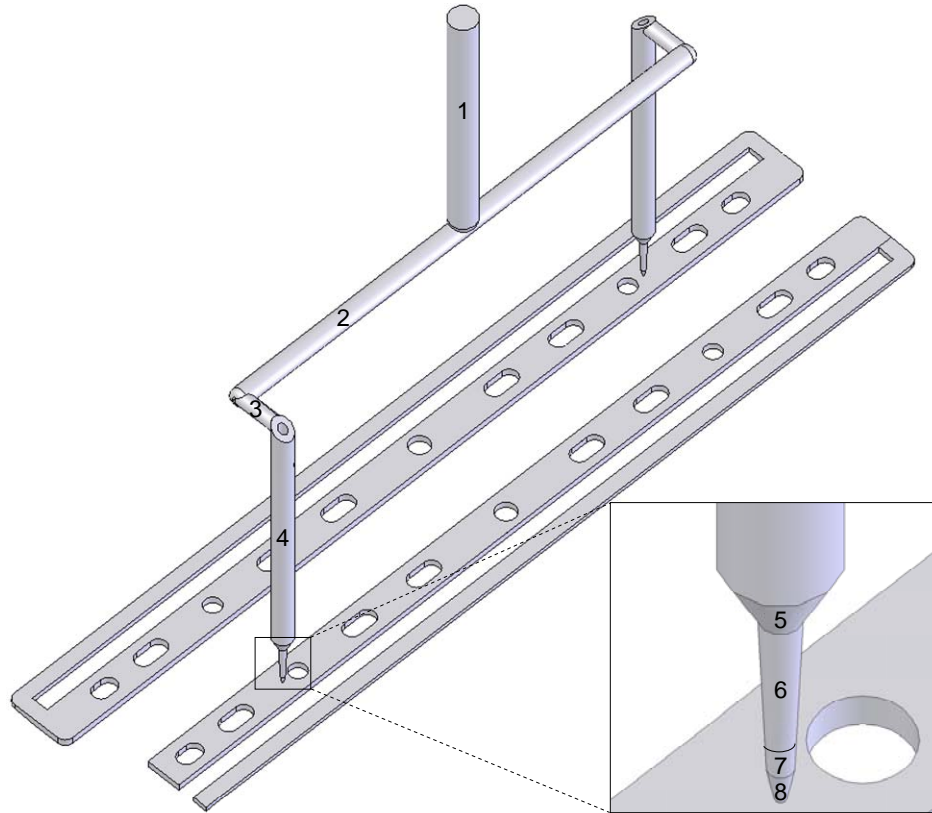


**Figure 2 Valve gate hot runner feed system and mold cavity geometry**

Fortunately, the dimensions of the feed system are known *a priori* so that the flow rates may be calculated *in situ* regardless of changes in the mold cavity geometry. The dimensions of the hot runner system for this application is listed in Table 1, where the segment numbers correspond to hot runner geometry shown in Figure 2. In the table,  $R_1$  is zero for a rod, and  $\delta$  indicates the percent reduction in  $R_2$  at the end of a tapered segment.

**Table 1 Geometries of the hot runner system**

The material used in the experiments is polypropylene (PP Borealis HF135M). The rheological property of the material was characterized on a capillary rheometer (Kayeness Inc. Model no. Galaxy V 8052) with a capillary length and diameter of 30 mm and 1 mm, respectively. The coefficients of the Cross-WLF model are listed in Table 2.

$L$	$R_1$
93	0
90	0
17	0
87.76	1.55
3.24	1.55
13	1.55

The experimental data and the fitted curves are shown in Figure 3.

**Table 2 Coefficients of the Cross-WLF viscosity model**

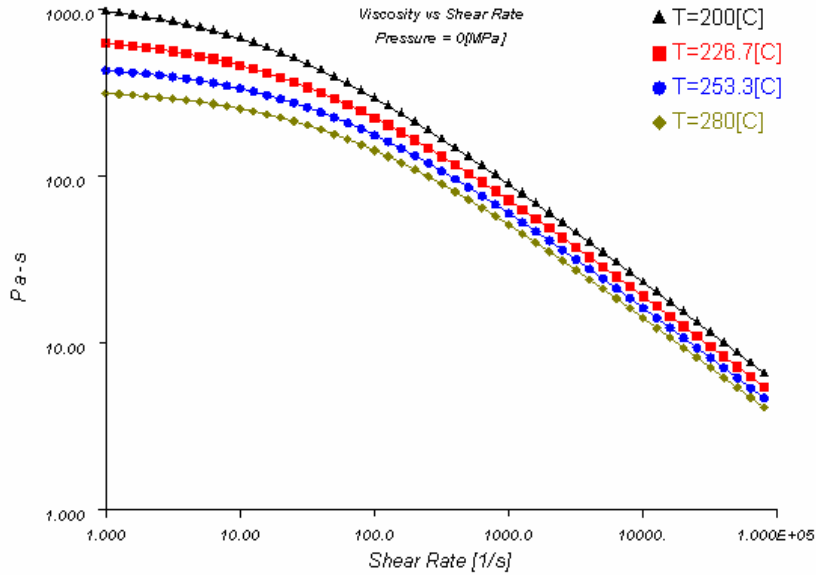


**Figure 3 Viscosity of PP: WLF model from MoldFlow**

The experiments were conducted on an HPM 80 ton tiebarless, hydraulic molding machine. According to supplier recommendations, the barrel temperature was profiled to supply a melt temperature of 215 C; the mold coolant temperature was regulated at 50 C. Different mold and process configurations were tested as summarized in Table 3.

**Table 3 Run Conditions**

Run	Cavity 1	Cavity 2	Filling	Packing	Melt Temp
1	Full Part	Full Part	100%	100%	215 C
2	Full Part	Full Part	50%	0%	215
3	Blocked End	Full Part	100%	100%	215
4	Blocked End	Full Part	50%	0%	215
5	Blocked End	Full Part	100%	100%	238

A first set of experimental runs was conducted in which the mold contained two full cavities. The molding process was setup so that the filling stage produced full parts with

$D_1$   
(PaSec)

$D_2$   
(K)

---

1.36e+12

263.15

a smooth transition to the packing stage. A short shot study was then conducted in which the shot size was reduced and the packing stage was not utilized. Afterwards, an insert in the mold was replaced to block one end of the one mold cavity to produce a partial binder part as shown in Figure 2. This second set of experimental runs was conducted at the same process settings as for the first set of runs with the full mold cavities. Due to the increased flow length, however, the cavity with the blocked end was not able to completely fill. An additional experimental run was then conducted with an increased melt temperature to investigate the effect of reduced melt viscosity on the flow rate and mass of the molded parts.

As previously stated, the objective of the implemented analysis is to estimate the flow rate to each mold cavity in real time, to thereby be able to predict quality attributes (such as weight, dimensions, etc.) before the mold opens and the part is ejected. Accordingly, it was not an objective of the above experiments to produce high quality parts, but rather to predict the quality of the molded parts from the process data and the described analysis. Accordingly, the mold was instrumented with piezoelectric load sensors (Kistler 9213) located behind ejector pins with a sensitivity corresponding to 4.1 pC/N force or 0.93 pC/MPa melt pressure. Per common industry practice, the injection pressure was estimated as the acquired hydraulic pressure multiplied by the machine's intensification ratio of 9.0. Screw position was also acquired from which the volumetric flow rate at the inlet was calculated.

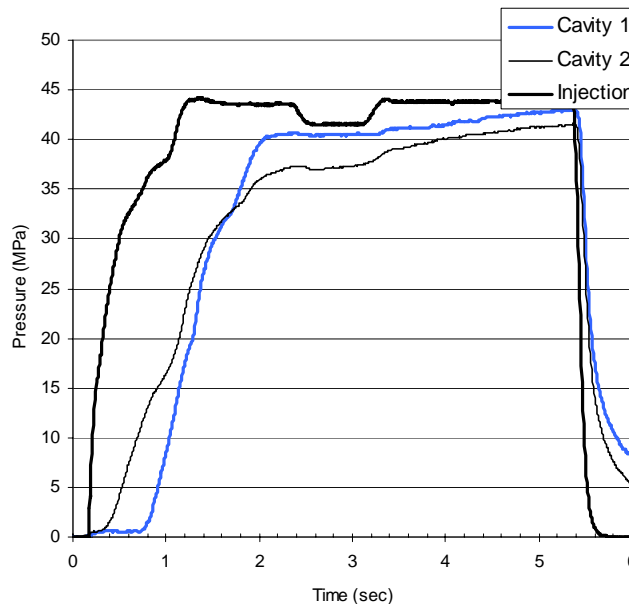


**Figure 4 Pressures for run 1**

A typical set of injection and cavity pressures for run condition 1 is shown in Figure 4. The injection pressure quickly increases from zero at 0.2 seconds to approximately 30 MPa at 0.4 seconds. This pressure increase is related to the pressurization of the polymer melt in the hot runner system when the valve gates are closed. After the valve gate for cavity two opens, the polymer melt propagates in the mold cavity, causing an increase in

the cavity pressure at the gate and a further increase in the injection pressure. At approximately 0.8 seconds, the valve gate for cavity one opens and the polymer melt propagates in the cavity as recorded by the pressure sensor. At approximately two seconds both cavities are full and a packing stage is provided in which the injection pressure is maintained at 44 MPa.

Injection and cavity pressure profiles are frequently used to track process repeatability and try to discern process events such as arrival of the melt, filling of the cavity, shrinkage, etc. The predicted mass flow rates based solely on the sensed pressure data, melt rheology, and feed system geometry are provided in Figure 5. As can be observed, the valve gate for cavity two opens prior to the valve gate for cavity one. The sudden opening of the valve gate for cavity one provides a surge of material into cavity one since the injection pressure is at a very high level. Furthermore, there is a slight drop off in the mass flow rate into cavity two due to the redirection of the melt into cavity one. At approximately two seconds, the cavities are full and the mass flow rate declines significantly.

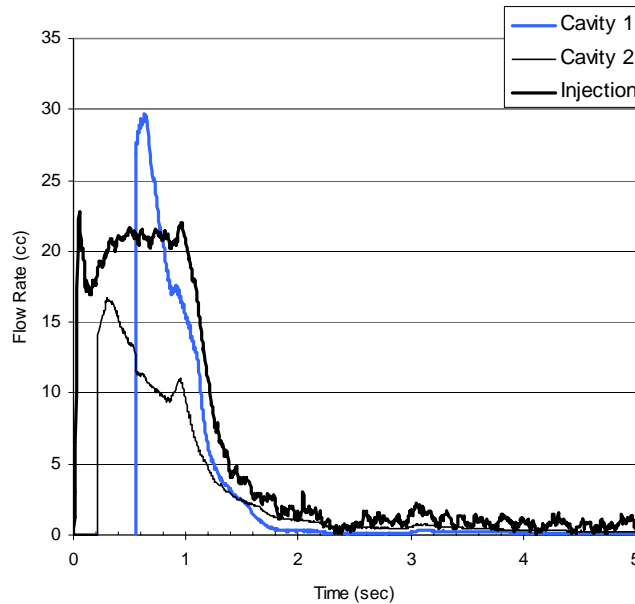


**Figure 5 Observed flow rate and predicted mass flow rates for run 1**

The pressure data and flow rate predictions are provided in Figure 6 for experimental run 3, in which the end of cavity one near the gate has been blocked off. In this case, the melt pressure in cavity one increases more quickly than for run one since the flow must be directed down the length of the part and back around into the thinner section. As a result, the simulation predicts a more rapid decrease in the flow rate for cavity one than for run 1.

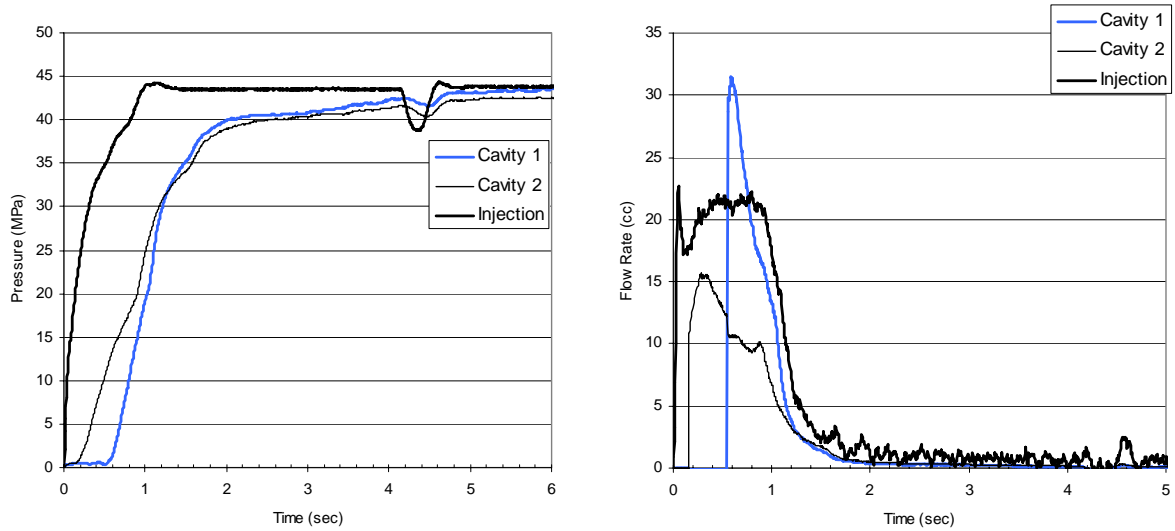


**Figure 6 Pressure data and predicted mass flow rates for run 3**

Similar analyses were conducted for all the experimental runs. The molded parts were weighted, which is the integral of the mass flow rate to each cavity. The measured and predicted part weights are shown in Table 4. As can be observed, there is a significant error between the predictions and the observed part weights.

**Table 4 Part Weight Comparison**

<i>Run</i>	<i>Cavity</i>	<i>Observed</i>	<i>Predicted</i>	<i>Error</i>
1	1	8.20g	12.68	55
	2	8.16	10.07	23
2	1	5.93	6.12	3
	2	3.66	4.23	16
3	1	8.29	11.16	35
	2	7.43	10.43	40
4	1	6.08	6.13	1
	2	3.23	4.54	41
5	1	8.17	8.87	9
	2	7.47	8.57	15

## Discussion

Herein begins an analysis of the variance. Errors may arise from the constitutive material models, the phenomenological models, the experimental conditions, and other sources. With respect to the material modeling, rheological data for this specific material was internally tested and fit to the Cross-WLF model. However, we note that the rheological model in the Moldflow database is significantly different than for our model and predicts significantly increased mass flow rates, which would tend to improve the results. Furthermore, the melt density (utilized to calculate the mass flow rate) was calculated using the Tait equation with coefficients from the Moldflow database. However, we note that the specific volume of the material at room and processing temperatures are 15%

higher than the values reported from the material supplier, which would tend to improve the results.

With respect to phenomenological models, the foregoing analysis assumes that the melt is incompressible with respect to the solution of the volumetric flow rates, though mass flow rate into the cavity is calculated according to the Tait equation. An inspection of the observed flow rate at the nozzle and predicted mass flow rates into the cavity are offset in time. In other words, the ram has started driving forward and pressurized the melt in the feed system prior to any flow into the cavity. Accordingly, it is clearly important to model the compressibility of the material for on-line simulation. There are a host of other possible phenomenological errors that may include but are not limited to viscoelasticity, orientation, acceleration dynamics, juncture losses, and others that the authors hope are not appreciable.

With respect to the experimental conditions, there are several known and suspected sources of error. First, the temperature of the polymer melt is not truly known. However, molding with a hot runner should mitigate this error since the melt resides in a nearly isothermal environment for about thirty seconds between the end of injection and subsequent start of injection. Second, the cavity pressure transducers are located approximately 10mm away from the gate, which corresponds to a few millisecond delay in the receipt of data and a slight decrease in the cavity pressure compared to the true (and unknown gate pressure). Some of the error due to the placement of the pressure sensor can be corrected by including a segment to model the area of the cavity between the transducer and the gate and then interpolating the upwind pressure at the gate. Third, the dynamic position of the valve pin in the drop of the hot runner is not known. While the valve pin actuators could be instrumented with position transducers, the increased cost and complexity would generally not be acceptable in industry applications. As a result, it is necessary to estimate the valve pin position based on the cavity pressure data and/or modeled actuator dynamics. It should be noted, moreover, that our ultimate goal is not only to predict the flow to each cavity but indeed to directly control it using the real time predictions from on-line simulations. Accordingly, the slow dynamics of the pneumatic actuators in this experimental investigation are clearly unsuitable for dynamic control of the valve gates.

These are just some of the errors, and there are very likely others. While such errors are common and accepted (or not apparent) with respect to product design and off-line process simulation, these errors severely limit the credibility and value of the on-line simulation with respect to quality prediction and control. In particular, it is not uncommon for part weights to be consistently controlled wherein the coefficient of variation (defined here as  $\sigma/\mu$ ) is less than 0.1%. Accordingly, it is vital that the on-line analysis contain on-line calibration to improve and correct predictions to the extent that is technically possible. Two very obvious corrections include mass conservation and on-line rheological characterization.

With respect to mass conservation, it is observed that approximately 15.9 g of polymer melt was injected into the mold cavities for runs 1, 3, and 5 (on average). However, the

simulation (based solely on rheological models and feed system geometry without modeling the compressibility effect on flow) predicted that approximately 22 g on average entered the cavities. Lack of mass conservation in these cases corresponds to a 40% error, which is the majority of the error listed in Table 4. Accordingly, current efforts are underway to develop and validate an improved on-line simulation which proportions the mass flow rate to each cavity in real time based on the volumetric flow rate feedback from the molding machine and the relative mass flow rates predicted in real time from the simulation. Unfortunately, such artificial mass conservation can cause errors from external sources such as leakage of the melt past the check-ring, leakage of the melt at the nozzle-sprue interface, and others.

With respect to on-line rheological characterization, it is our philosophy that improved rheological modeling will provide improved results. However, please consider that the Newtonian model has one coefficient, the power law model has two coefficients, the Ellis model has three coefficients, an Ellis model with Arrhenius temperature dependence has four coefficients, and the Cross model with WLF temperature dependence has six coefficients (not including pressure dependence). As the number of model coefficients increases, the behavior of the melt is better modeled. However, the increased number of model coefficients significantly complicates the on-line rheological characterization. One approach is to assume only a power law index and temperature sensitivity for a given material, thereby requiring on-line characterization of a reduced number of rheological parameters e.g. the Newtonian limit and the critical shear stress.

Further corrections to the on-line simulation are possible, though of debatable merit. For instance, it is possible to require a design of experiments to calibrate the model on-line, and then correct the simulation results using an expert system and/or look-up tables. Such an empirical approach (without the on-line simulation) was previously implemented [31-34] but found to require too extensive an experimental investigation and part quality characterization by molders on an application basis. Alternatively, it is possible to utilize the results of the on-line simulation along with the process data to train and operate a neural network. Such a hybrid neural network approach (without the on-line simulation) was previously implemented [20, 35-37] but also found to require too extensive a training run without significant insights into the process. Furthermore, both these corrective approaches are highly susceptible to external variation in which an external variable can render the empirical models valueless. Accordingly, the authors opine that on-line simulations should be based on physics rather than empirical observations.

The described analysis has been implemented in ANSI C and MS/Visual Basic. The solution time for  $n$  segments is of the order  $(n+n^2)$ . The linear term is driven by the solution of the temperature field (which involves the inversion of a tri-diagonal matrix) and integration of the flow conduction for each segment. The second order term is driven by the inversion of the flow conductance matrix. Our objective was to develop an implementation with a solution time of less than 2 mSec for a sixteen cavity system, which could be directly incorporated into machine controllers with controller sweep times on this time scale. The estimated CPU times are listed in Table 5 as a function of  $n$  for a 2.4 GHz Pentium 4 computer.

**Table 5 Solution time**

<i>n</i>	<i>t (mSec)</i>
1	0.06
2	0.13
4	0.29
8	0.69
16	1.8
32	5.4
64	18
128	64
256	242
512	937

This data indicates the feasibility of performing on-line simulation with up to 64 segments with a solution time of less than 20 mSec. While 2.4GHz computers are common on the desktop, the computers found in controllers are typically half the speed of new desktop computers (due in large part to delays in controller development time and/or lengthy testing requirements). Furthermore, only a fraction of the CPU time is available on most controllers since the controller must also control the process, interface with the operator, etc. As such, the current simulation is likely appropriate for only 32 or even 16 segments. If a higher number of segments are required, then a parallel processing scheme or improved solution approach is required.

Analytical and quasi-analytical solutions have existed in the literature or have been developed by the authors for the Newtonian, power law, Ellis models, and non-isothermal Ellis models. These analytical approaches have the advantage of immediate construction of the flow conductance matrix. Our research indicates that it is important to capture the shear-dependence of the viscosity. Furthermore, our research indicates that there can be significant shear heating in the feed system. As a result, we have developed but not yet validated a quasi-analytical solution for a non-isothermal Ellis model in which the bulk temperature of the melt is estimated by a balance of the heat convection, viscous generation, and heat conduction terms. The authors are currently disputing the relative merit of this approach given the solution time of the previously described analysis. However, it is possible that the suggested quasi-analytical approach may provide sufficiently accurate results and significantly reduced solution times with a forward propagation scheme that avoids the inversion of the flow conductance matrix.

## **Conclusions**

A flow network analysis is presented with the capability of the estimating pressure and flow rate for a non-Newtonian, non-isothermal flow. The error of the predicted part weights with the measured parts range from 3% to 55%. The primary source of error is presumably the lack of mass conservation between the physical system and the simulated system. Other significant error sources include the rheological model and known equipment issues. With the finite difference calculation of the energy equation and the

flow network analysis, the simulation runs reasonably fast. The execution time of the simulation with 16 flow segments is less than 2 mSec per time step.

The reported results and related discussion clearly indicate that this first implementation of on-line flow simulation is not ready for industry use. However, this implementation has provided the authors great insight, such that the required improvements are well defined and the second implementation is underway. It is our continued belief that on-line simulation provides a significant opportunity for *in situ* prediction and control of unobservable process states such as melt viscosity, flow rate, shrinkage, density, stress, and others. If successful, a new generation of machine controllers can be enabled that provides better information to the operator, increased ease of use, and (most of all) increased process capabilities.

## Acknowledgements

Portions of this work were funded by Mold-Masters Ltd. Of Georgetown, Ontario and the National Science Foundation Division of Design, Manufacturing, and Industrial Innovation, Grant No. 02-045309. The contents of this paper do not represent the opinions of Mold-Masters Ltd., the National Science Foundation, or the United States Government.

## References

- [1] D. O. Kazmer, "Precision Process Control," in *Precision Injection Molding*, J. Greener, Ed.: Hanser, 2004.
- [2] J. W. Mann, "Process Parameter Control: the Key to Optimization," *Plastics Engineering*, vol. 30, pp. 25-27, 1974.
- [3] M. R. Kamal, W. I. Patterson, N. Conley, D. Abu Fara, and G. Lohfink, "Dynamics and Control of Pressure in the Injection Molding of Thermoplastics," *Polymer Engineering and Science*, vol. 27, pp. 1403-1410, 1987.
- [4] F. Gao, I. A. N. Patterson, and M. R. Kamal, "Self-tuning cavity pressure control of injection molding filling," *Advances in Polymer Technology*, vol. 13, pp. 111-120, 1994.
- [5] S. L. B. Woll and D. J. Cooper, "Pattern-based closed-loop quality control for the injection molding process," *Polymer Engineering and Science*, vol. 37, pp. 801-812, 1997.
- [6] L.-J. Chien, C. L. Thomas, and D. R. Lawson, "Sensor/model fusion for improved process understanding and control in injection molding," presented at CAE and Intelligent Processing of Polymeric Materials, Dallas, TX, 1997.
- [7] P. D. Coates, A. R. Haynes, and R. G. Speight, "In-line characterization of polymer deformation in melt and solid phase processing," *Polymer*, vol. 35, pp. 3831-3843, 1994.
- [8] R. Trim, "On-line quality control," *British Plastics and Rubber*, pp. 18-19, 1997.
- [9] C. T. Burke and D. O. Kazmer, "Experimental comparison of state of the art high shear rate polymer rheological characterization techniques," presented at Proceedings of the 52nd Annual Technical Conference ANTEC, Part 1 (of 3), 1994.

- [10] D. H. Harry and R. G. Parrott, "Numerical Simulation of Injection Mold Filling," vol. 10, pp. 209-14, 1970.
- [11] K. K. Wang, "System Approach to Injection Molding Process," presented at Annual Technical Conference of the Society of Plastics Engineers, New Orleans, LA, 1979.
- [12] V. G. Gomes, W. I. Patterson, and M. R. Kamal, "Injection Molding Study: Evaluation of Alternative Control Strategies For Melt Temperature," *Polymer Engineering and Science*, vol. 26, pp. 867-876, 1986.
- [13] H. H. Chiang, "Simulation and Verification of Filling and Post-Filling Stages of the Injection-Molding Process," Ph.D. Dissertation, Cornell University, 1989.
- [14] K. Himasekhar, K. K. Wang, and J. Lottey, "Mold-cooling simulation in injection molding of three-dimensional thin plastic parts," presented at American Society of Mechanical Engineers, Heat Transfer Division, (Publication) HTD, Philadelphia, PA., 1989.
- [15] Hwai Hai Chiang, "Simulation and Verification of Filling and Post-Filling Stages of the Injection Molding Process," in *Mechanical Engineering*. Ithaca, NY: Cornell University, 1989.
- [16] K. K. Wang, "Twenty years of CIMP research towards CAE for injection molding," presented at International Mechanical Engineering Congress and Exposition Materials Division, Advances in Computer-Aided Engineering (CAE) of Polymer Processing, Chicago, IL, 1994.
- [17] J. P. Coulter, E. E. Higuerey, J. M. Troiano, H. H. Demirci, and T. L. Nixon, "Real time sensing of resin flow dynamics during intelligent molding," *Journal of Materials Processing and Manufacturing Science*, vol. 5, pp. 173-181, 1997.
- [18] D. Kazmer and P. Barkan, "Multi-cavity pressure control in the filling and packing stages of the injection molding process," *Polymer Engineering & Science*, vol. 37, pp. 1865-1879, 1997.
- [19] S. Orzechowski, A. Paris, and C. J. B. Dobbin, "Process monitoring and control system for injection molding using nozzle-based pressure and temperature sensors," presented at Annual Technical Conference - ANTEC, Conference Proceedings, 1998.
- [20] T. Petrova and D. Kazmer, "Development of a hybrid neural network for quality control of injection molding," presented at Proceedings of the 56th Annual Technical Conference, ANTEC, Part 1 (of 3), 1998.
- [21] C. M. Seaman, A. A. Desrochers, and G. F. List, "Multiobjective optimization of a plastic injection molding process," *IEEE Transactions on Control Systems Technology*, vol. 2, pp. 157-168, 1994.
- [22] H. Chipman, "Handling uncertainty in analysis of robust design experiments," *Journal of Quality Technology*, pp. 11-17, 1998.
- [23] J. Y. A. U. Park and K. Behrokh, "Real-time computer-aided process planning system as a support tool for economic product design," *Journal of Manufacturing Systems*, vol. 12, pp. 181-193, 1993.
- [24] R. K. Irani, S. Kodiyalam, and D. O. Kazmer, "Runner system balancing for injection molds using approximation concepts and numerical optimization," presented at 18th Annual ASME Design Automation Conference, Scottsdale, AZ, USA, 1992.

- [25] G. Sherbelis, E. Garvey, and D. Kazmer, "Methods and benefits of establishing a Process Window," presented at Proceedings of the 55th Annual Technical Conference, ANTEC, Part 1 (of 3), 1997.
- [26] Z. Tadmor and C. G. Gogos, *Principles of Polymer Processing*: John Wiley & Sons, 1979.
- [27] J. Agassant, P. Avanas, J. Sergent, and J. Garreau, *Polymer Processing: Principles and Modeling*, 1991.
- [28] D. O. Kazmer, B. Fan, and R. Najeri, "On-Line Flow Rate and Pressure Analysis with Sensor Fusion," presented at Society of Plastics Engineers Annual Technical Conference, Chicago, IL, 2004.
- [29] B. Fan, D. O. Kazmer, W. C. Bushko, R. P. Theriault, and A. J. Poslinski, "Simulation of Injection-Compression Molding for Optical Media," *Polymer Engineering & Science*, vol. v. 43, pp. 596-606, 2003.
- [30] H. H. Chiang, C. A. Hieber, and K. K. Wang, "A Unified Simulation of the Filling and Postfilling Stages in Injection Mold. Part I: Formulation," *Polymer Engineering and Science*, vol. 31, pp. 116-124, 1991.
- [31] D. Kazmer, J. Rowland, and G. Sherbelis, "Foundations of intelligent process control for injection molding," *Journal of Injection Molding Technology*, vol. 1, pp. 44-56, 1997.
- [32] J. C. Rowland and D. O. Kazmer, "On-line quality monitoring system for thermoplastic injection molding," presented at Proceedings of the 54th Annual Technical Conference, Part 1 (of 3), 1996.
- [33] J. C. Rowland and D. O. Kazmer, "Quantifying the economic value added of on-line quality control systems," presented at Proceedings of the 55th Annual Technical Conference, ANTEC, Part 1 (of 3), 1997.
- [34] R. Thomas, J. Rowland, and D. Kazmer, "On-line injection-control systems ace the value test," *Modern Plastics*, vol. 74, pp. 83-84, 86, 1997.
- [35] D. O. Kazmer and T. Petrova, "Synthesis and analysis of quality control methods for intelligent processing of polymeric materials," presented at Proceedings of the ASME International Mechanical Engineering Congress and Exposition, Dallas, TX, USA, 1997.
- [36] T. T. Petrova and D. O. Kazmer, "Hybrid Neural Models for Pressure Control in Injection Molding," *Advances in Polymer Technology*, vol. 18, pp. 1-13, 1999.
- [37] T. Petrova and D. Kazmer, "Incorporation of phenomenological models in a hybrid neural network for quality control of injection molding," *Polymer-Plastics Technology & Engineering*, vol. 38, pp. 1-18, 1999.